Electronic supplementary information (ESI)
for

Chirality Transfer in a Cage Controls the Clockwise / Anticlockwise Propeller-like Arrangement of the tris(2-pyridylmethyl)amine Ligand

Gege Qiu, [a] Cédric Colomban,*[a] Nicolas Vanthuyne,[a] Michel Giorgi,[b] and Alexandre Martinez *[a]

a. Aix Marseille Univ, CNRS, Centrale Marseille, iSm2, Marseille, France.
E-mail: alexandre.martinez@centrale-marseille.fr ; cedric.colomban@univ-amu.fr
b. Aix Marseille Univ., CNRS, FSCM, Spectropole, Marseille, France

Table of contents:

1. Chemical and instrumentation

All reagents were commercial reagent grade and were used without further purification. **$TPACl_3$,**[S1] and **$CTV(OH)_3$,** [S2] (were obtained according to reported protocols.

Instrumentation

^1H NMR and ^{13}C NMR were recorded on a Bruker Avance III HD 300 MHz and 500MHz spectrometers. ^1H NMR and ^{13}C NMR chemical shifts δ are reported in ppm referenced to the protonated residual solvent signal. ESI-HRMS were performed on a SYNAPT G2 HDMS (Waters) mass spectrometer with API and spectra were obtained with TOF analysis. Measurements were realized with two internal standards. Electronic Circular Dichroism. ECD and UV spectra were measured on a JASCO J-815 spectrometer equipped with a JASCO Peltier cell holder PTC-423 to maintain the temperature at 25.0 ± 0.2°C. A CD quartz cell of 1 mm of optical pathlength was used. The CD spectrometer was purged with nitrogen before recording each spectrum, which was baseline subtracted.The baseline was always measured for the same solvent and in the same cell as the samples.The spectra are presented without smoothing and further data processing

2. Experimental procedure and characterisation

Synthetic procedure for 1

To a solution of **$CTV(OH)_3$** (408 mg, 1 mmol) and **$TPA(Cl)_3$** (440mg, 1.03 eq) in DMF(350 mL), Cs_2CO_3 (500 mg) was added in one portion. Then the solution was stirred overnight at 90°C under argon. The mixture was then allowed to return to room temperature, evaporated and water was added (200 mL). The aqueous mixture was extracted with CH_2Cl_2 (3x 100 mL). The combined organic phases were washed with 1M aqueous NaOH (100 mL), washed with brine (100 mL), dried over Na_2SO_4, filtered and evaporated to dryness. The residue was purified purified by column chromatography on silica (eluent : CH_2Cl_2 / CH_3OH; 12:1) to afford a white solid. Yield: 66%. ^1H NMR (300 MHz, $CDCl_3$) δ ppm: 7.59 (t, J = 7.6 Hz, 3H, PyH), 7.26 (s, 3H, PyH), 7.04 (d, J = 7.6 Hz, 3H, PyH), 6.34 (s, 3H, ArH), 6.27 (s, 3H, ArH), 5.36 (d, J = 12.8 Hz, 3H,OCH_2Py), 5.25 (d, J = 12.8 Hz, 3H,OCH_2Py), 4.44 (d, J = 13.7 Hz, 3H, $ArCH_2Ar$), 3.72 (s, 9H, OCH_3), 3.30 (d, J = 14.0 Hz, 3H, $PyCH_2N$), 3.21 (d, J = 13.8 Hz, 3H, $ArCH_2Ar$), 2.64 (d, J = 14.1 Hz, 3H, $PyCH_2N$). HRMS (ESI, [M + H]+): m/z: calcd for for $C_{45}H_{42}N_4O_6$ 735.3104, found 735.3165. ^{13}C NMR (101 MHz, 298K, $CDCl_3$): δ ppm: 159.14, 154.47, 149.63, 144.80, 136.11, 133.72, 131.29, 124.00, 120.52, 120.44, 113.63, 71.80, 57.00, 56.22, 36.26.

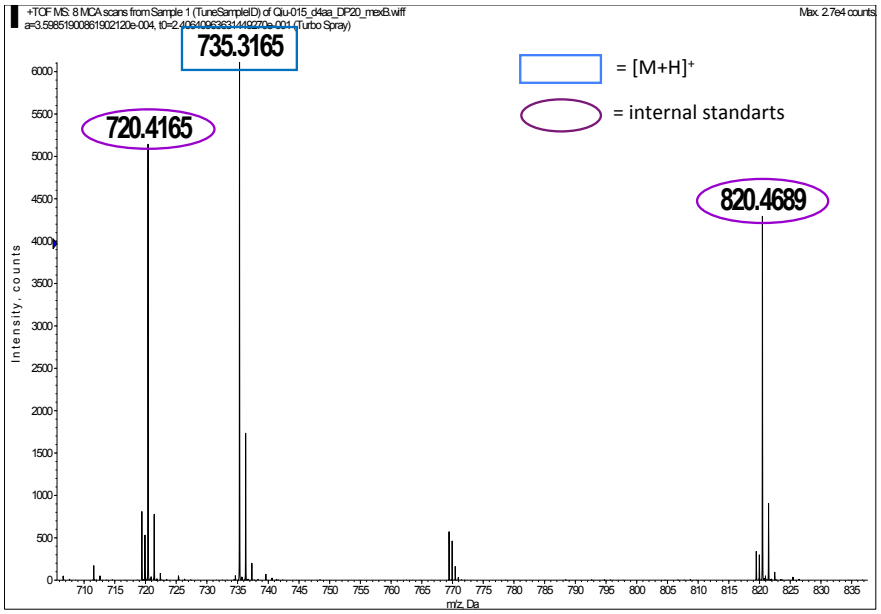

Spectra S1. ESI-HRMS spectra of **1** in CH_2Cl_2 / MeOH. The isotopic pattern at m/z = 735.3165 can be attributed to **1**.H+ ($m/z_{\text{calculated}}$ = 735.3104).

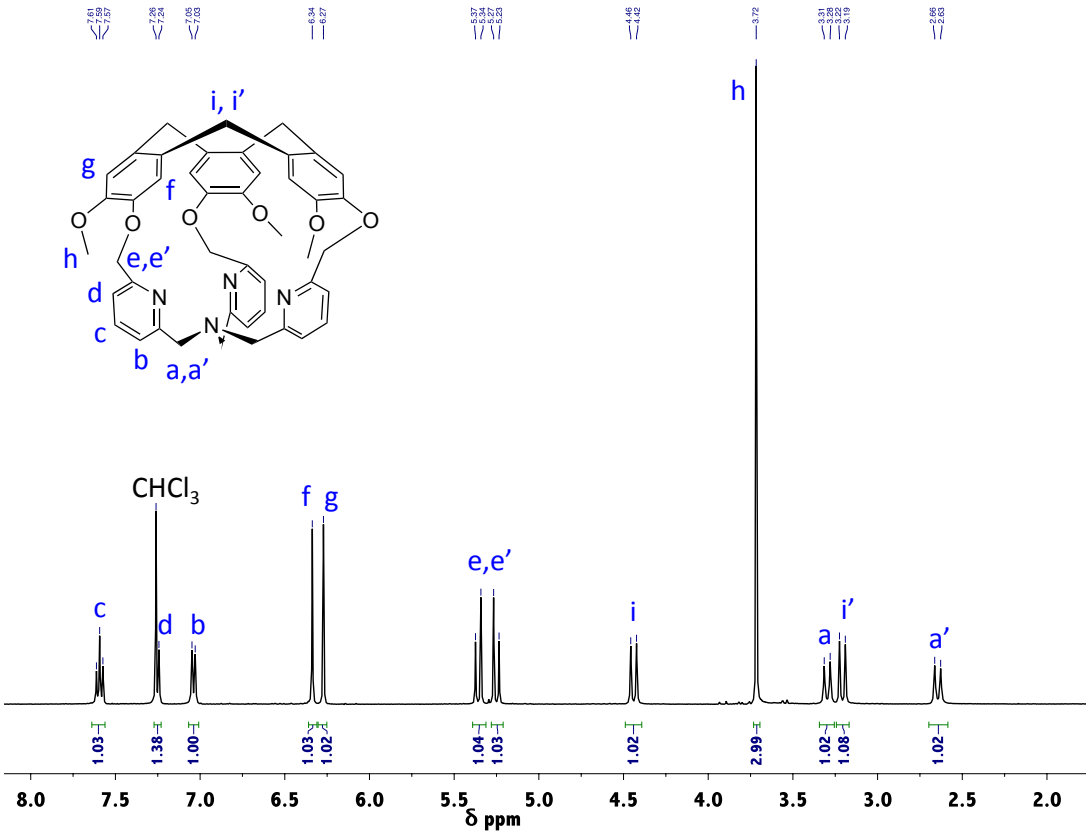

Spectra S2. ^{1}H-NMR spectra ($CDCl_3$, 300 MHz) of hemicryptophane **1**, at 298K

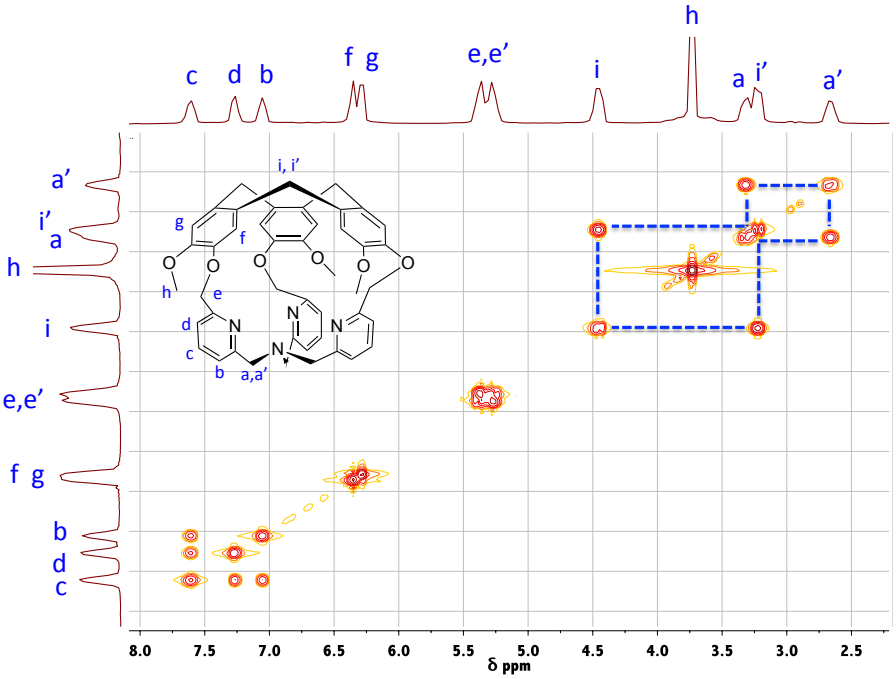

Spectra S3. 2D COSY-NMR spectra ($CDCl_3$, 300MHz) of **1** in $CDCl_3$, at 298K

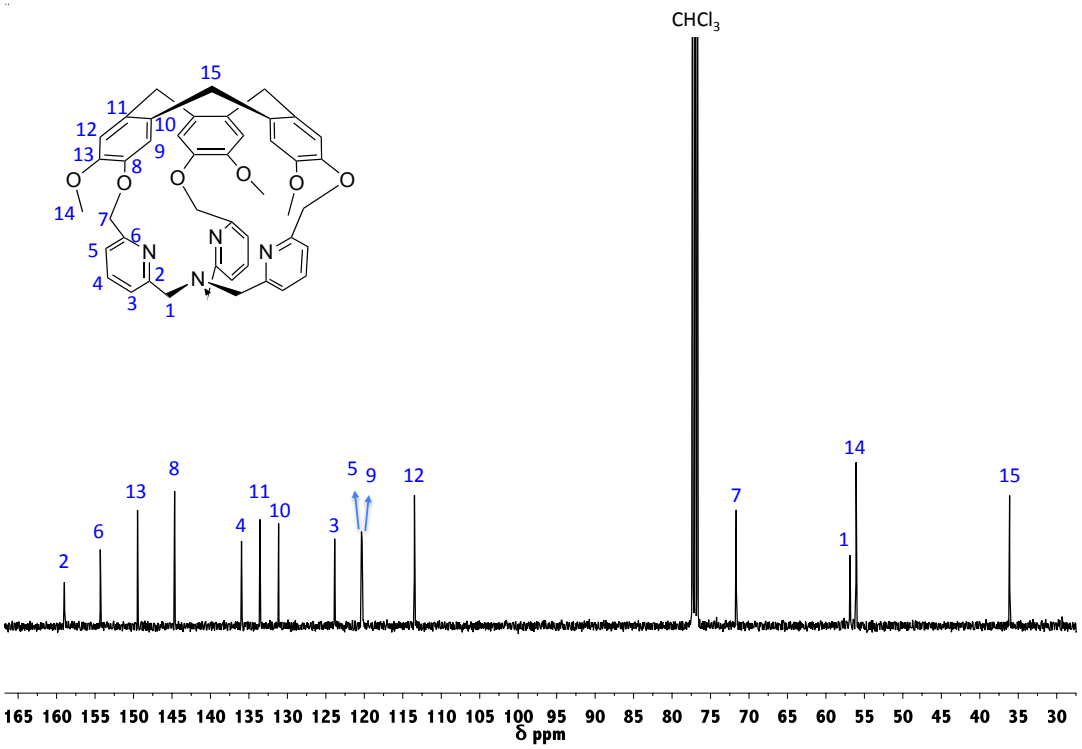

Spectra S4. ^{13}C-NMR spectra ($CDCl_3$, 101 MHz) of **1** in $CDCl_3$, at 298K.

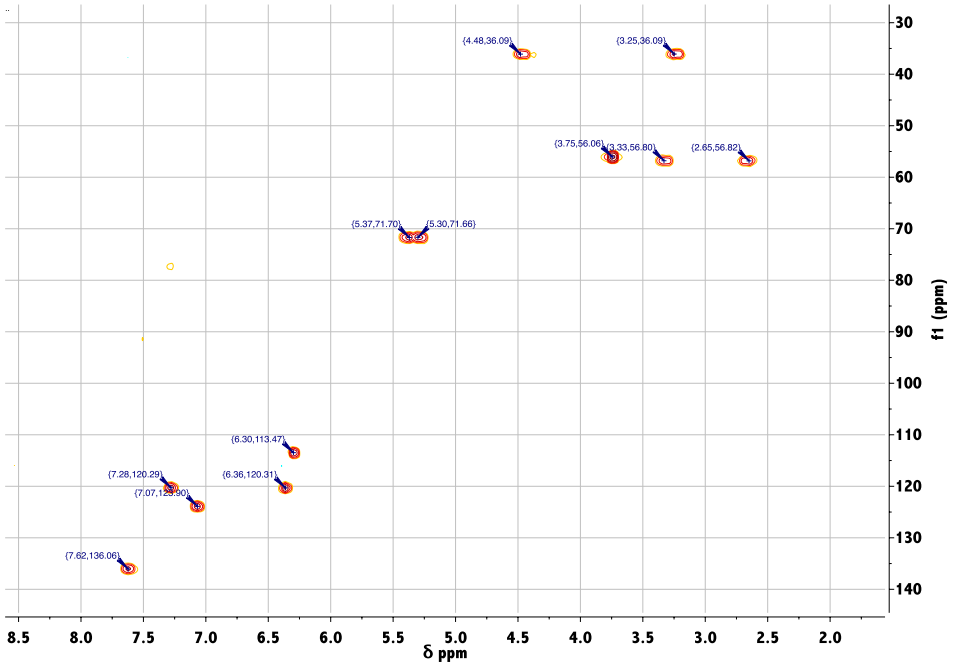

Spectra S5. ^{1}H-^{13}C HSQC-NMR spectra ($CDCl_3$, 300MHz) of **1** in $CDCl_3$, at 298K

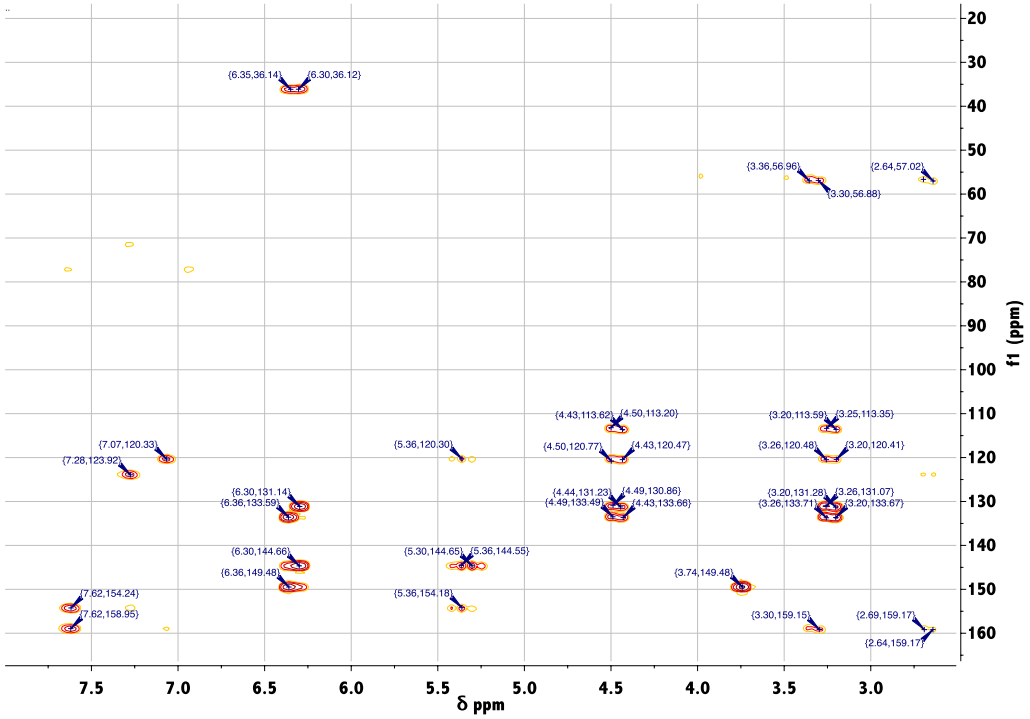

Spectra S6. ^{1}H-^{13}C HMBC-NMR spectra ($CDCl_3$, 300MHz) of **1** in $CDCl_3$, at 298K

Synthetic procedure for [1.H]-Cl

Protonation of the tertiary amine of **1** was achieved through its treatment with concentrated HCl in a CH_2Cl_2/CH_3OH solvent mixture, resulting in the formation of the protonated racemate **[1.H]-Cl**. Purity of the resulting adduct was further confirmed through ^{1}H-NMR and X-Ray diffraction studies. The ^{1}H-NMR spectrum of **[1.H]-Cl** (298K, $CDCl_3$) display, on average, a C_3 symmetrical structure with the characteristic signal of the quaternary H-N+ resonating at 12.00 ppm (Spectra S5). Compared to **1**, **[1.H]-Cl** display downfield shifted signal for the proton belonging to the pyridine (Hb, Hc, Hd) and the methylene HN+-CH_2 (Ha,a'). Proton belonging to the CTV unit (Hh, Hg, Hf, Hi,i') were less affected, confirming that the protonation takes place at the southern part of the molecule. Interestingly, the methylene protons (-CH_2-) at the alpha position of the quaternary amine of TPA (Ha/a' resonating at 4.11 and 3.21 ppm) remain diastereotopic with a gap of 0.9 ppm.

Single crystals of **[1.H]-Cl**, suitable for X-ray diffraction, were obtained by slow diffusion of Et_2O to a solution of cage in CH_2Cl_2 / MeOH. It display an asymmetric unit containing two of each *M*- and *P*- enantiomers of **[1.H]-Cl** (Fig. S9). For both enantiomers identical distances between the quaternary ammonium proton N+-H and the chlorine atom are observed (DN-H--Cl= 2.104 Å, ΘN-H—Cl = 153.29°), indicating for H-bonding interactions. It should be noted that, in both cases, the chlorine anion is engaged in a second hydrogen bond with an exogeneous molecule of methanol (DO-H--Cl = 2.440 Å, ΘO-H—Cl = 159.47°, see Figure S9).

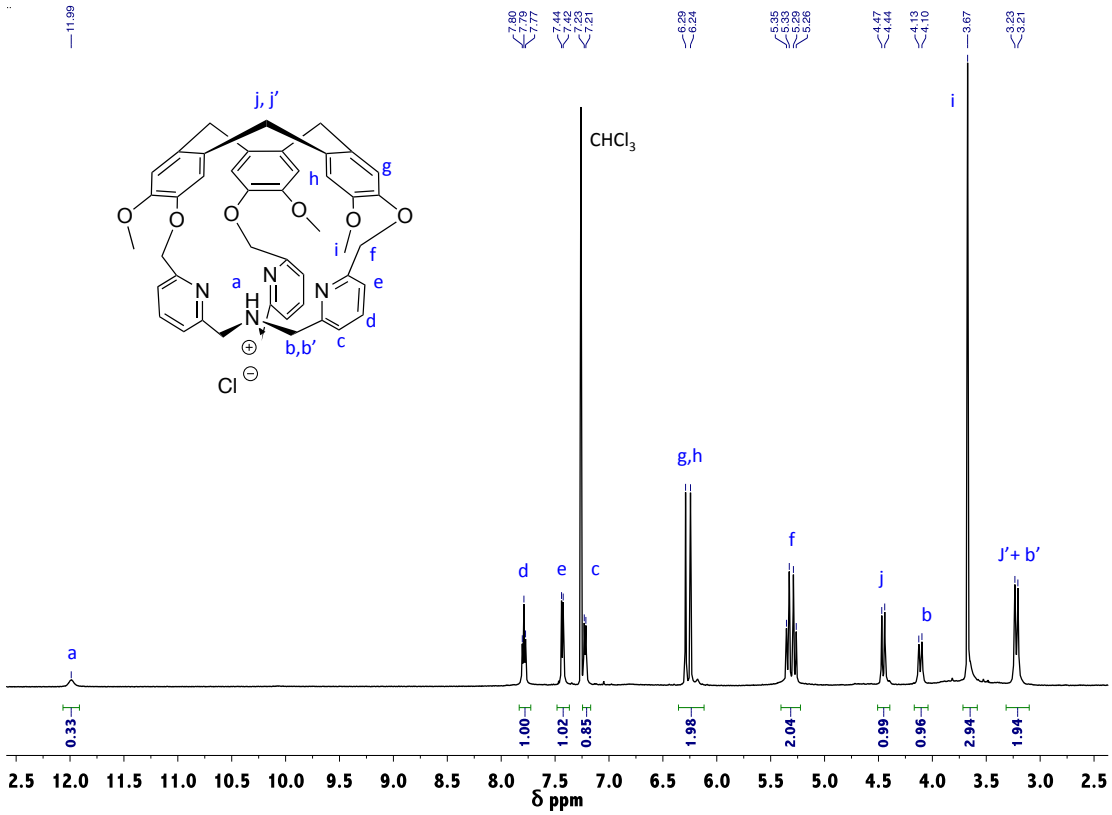

Spectra S7. ^{1}H-NMR spectra ($CDCl_3$, 300 MHz) of [**1.H]-Cl**, at 298K

Synthetic procedure for $Cu^{I}(1)(Cl)$

CuCl (1.35 mg, 0,0136 mol, 1.0 equiv.) was added, at room temperature to a stirred solution of **1** (10 mg, 0.0136 mmol, 1.0 equiv.) in THF (2 mL). The metallation occurred immediately and a pale yellow solid precipitated within minutes. The resulting pale yellow solid was isolated by filtration, washed with THF and dried in vacuo to give **$Cu^{I}(1)(Cl)$** in a 88% yield. ^{1}H-NMR spectrum of **$Cu^{I}(1)(Cl)$** at 298K display broad signals while its spectrum recorded at 260K gives well-defined and sharp signals (Spectra S6, figure S10). HRMS (ESI, $[M + Na]^{+}$): m/z calcd for $C_{45}H_{42}N_4O_6CuClNa$ 855.1981 found 855.1985. ^{1}H NMR (500 MHz, $CDCl_3$, 260K) δ ppm: 8.47 (d, 1H, PyH), 7.91 (m, 1H, PyH), 7.82 (t, 1H, PyH), 7,60 (t, 1H, PyH), 7,54 (d, 1H, PyH), 7,35 (d, 1H, PyH), 7.30 (d, 1H, PyH), 7.06 (broad, 1H, PyH), 6.94 (d, 1H, PyH), 6.45 (s, 1H, ArH), 6.36 (s, 1H, ArH), 6.12 (s, 1H, ArH), 6.01 (s, 1H, ArH), 5.88 (d, 1H, OCH_2Py), 5.76 (s, 1H, ArH), 5.72 (d, 1H, OCH_2Py), 5.47 (d, 1H, OCH_2Py), 5.35 (d, 1H, OCH_2Py), 5.31 (s, 1H, ArH), 4.98 (d, 1H, OCH_2Py), 4.84 (d, 1H, OCH_2Py), 4,45 (d, 1H, $ArCH_2Ar$), 4,30 (t, 2H, $ArCH_2Ar$), 3.93 (s, 3H, OCH_3), 3.78 (s, 3H, OCH_3), 3.73 (d, 1H, $PyCH_2N$), 3.71 (br s, 1H, $PyCH_2N$), 3.63 (d, 1H, $PyCH_2N$), 3.55 (s, 3H, OCH_3), 3.22 (m, 2H, $ArCH_2Ar$), 2.99 (d, 1H, $ArCH_2Ar$), 2.79 (d, 1H, $PyCH_2N$), 2.34 (d, 1H, $PyCH_2N$), 0.30 (d, 1H, $PyCH_2N$).

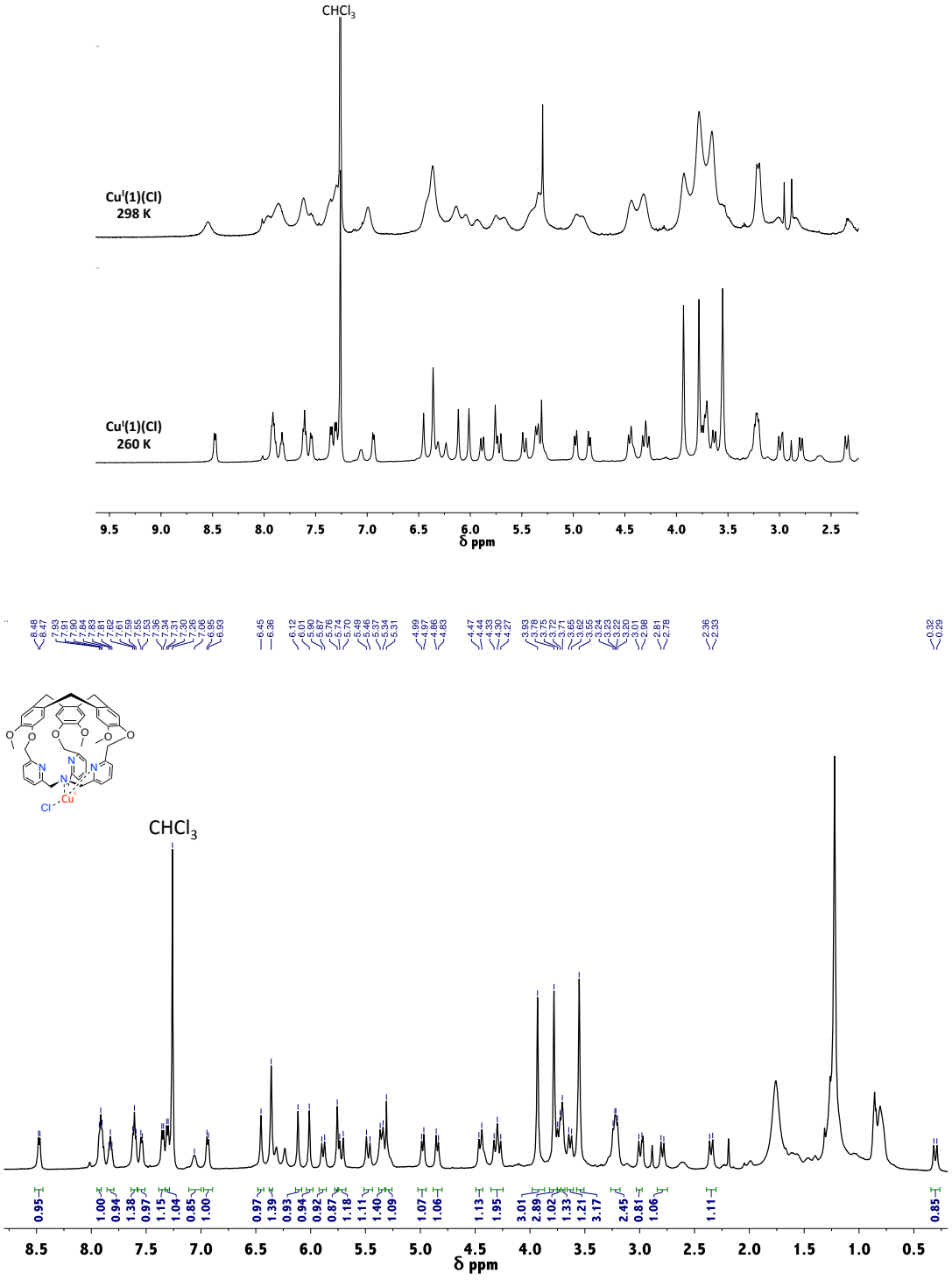

Spectra S8. Comparison of the ^{1}H-NMR spectra of **Cu^{I}(1)(Cl)**, at 298k and 260K. (Top). ^{1}H-NMR spectra ($CDCl_3$, 500 MHz) of **Cu^{I}(1)(Cl)**, at 260K (bottom), all signals corresponding to protons of **Cu^{I}(1)(Cl)** (integrated signals), have been assigned accordingly to the 2D COSY NMR experiment (spectra S9).

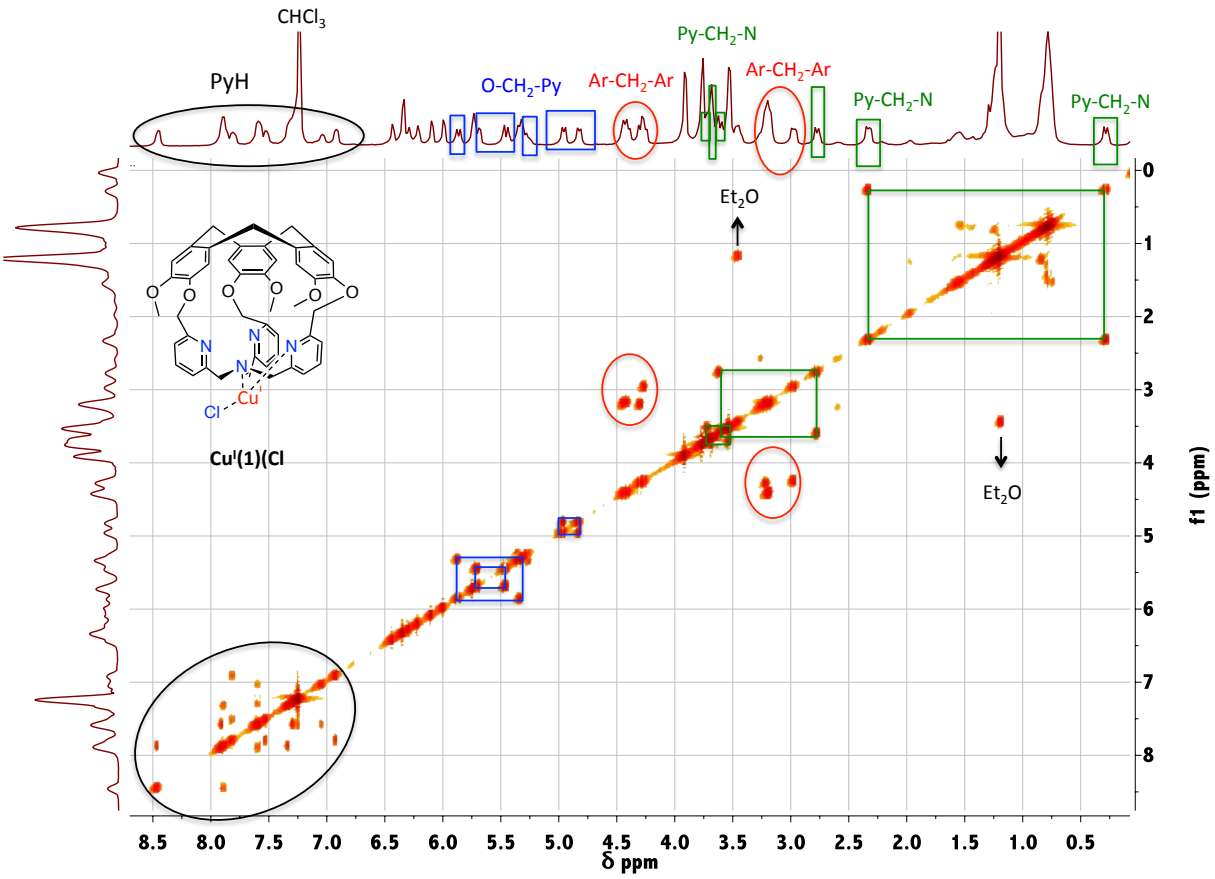

Spectra S9. 2D COSY-NMR spectra ($CDCl_3$, 300MHz) of **Cu^{I}(1)(Cl)** in $CDCl_3$, at 260K.

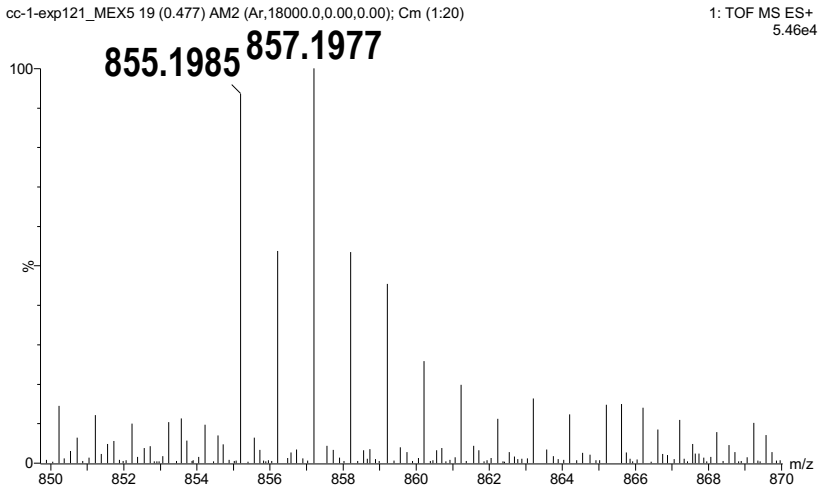

Spectra S10. ESI-HRMS spectra of **Cu^{I}(1)(Cl)** in CH_2Cl_2 / MeOH. The istopic pattern at m/z = 855.1985 can be attributed to **Cu^{I}(1)(Cl)**.Na+ ($m/z_{\text{calculated}}$ = 855.1981).

Single crystal X-ray Diffraction Data

- **1** (CCDC 1951499)

Single crystals of $C_{45}H_{42}N_4O_6$ (**1**) were crystallized by slow diffusion of Et_2O in a CH_2Cl_2 solution of the compound. A suitable crystal was selected and mounted on a SuperNova, Dual, Cu at home/near, AtlasS2 diffractometer. The crystal was kept at 253.00(10) K during data collection. Using Olex2, [S3] the structure was solved with the ShelXT, [S4] structure solution program using Intrinsic Phasing and refined with the ShelXL, [S5] refinement package using Least Squares minimisation.

Empirical formula	C45H42N4O6
Formula weight	734.82
Temperature/K	253.00(10)
Crystal system	monoclinic
Space group	$P2_1/c$
a/Å	10.02810(10)
b/Å	18.2669(2)
c/Å	20.2604(2)
β/°	98.4730(10)
Volume/Å3	3670.84(7)
Z	4
ρcalcg/cm3	1.330
μ/mm-1	0.718
F(000)	1552.0
Crystal size/mm3	0.14 × 0.12 × 0.06
Radiation	CuKα (λ = 1.54184)
2Θ range for data collection/°	6.548 to 142.092
Index ranges	-12 ≤ h ≤ 11, -22 ≤ k ≤ 21, -24 ≤ l ≤ 23
Reflections collected	34483
Independent reflections	7044 [Rint = 0.0231, Rsigma = 0.0159]
Data/restraints/parameters	7044/0/499
Goodness-of-fit on F2	1.041
Final R indexes [I>=2σ (I)]	R1 = 0.0468, wR2 = 0.1246
Final R indexes [all data]	R1 = 0.0530, wR2 = 0.1302
Largest diff. peak/hole / e Å-3	0.41/-0.29

- **[1.H]-Cl** (CCDC 1951501)

Single crystals of $C_{46}H_{47}ClN_4O_7$ **([1.H]-Cl**) were crystallized by slow diffusion of Et_2O in a CH_2Cl_2 / MeOH solution of the compound. A suitable crystal was selected and mounted on a SuperNova, Dual, Cu at home/near, AtlasS2 diffractometer. The crystal was kept at 295 K during data collection. Using Olex2, [S3] the structure was solved with the ShelXT, [S4] structure solution program using Intrinsic Phasing and refined with the ShelXL, [S5] refinement package using Least Squares minimisation.

Empirical formula	$C_{46}H_{47}ClN_4O_7$
Formula weight	803.32
Temperature/K	295
Crystal system	monoclinic
Space group	$P2_1/c$
a/Å	20.7019(2)
b/Å	10.84040(10)
c/Å	17.9416(2)
β/°	101.3700(10)
Volume/Å3	3947.38(7)
Z	4
ρcalcg/cm3	1.352
μ/mm-1	1.340
F(000)	1696.0
Crystal size/mm3	0.22 × 0.18 × 0.12
Radiation	CuKα (λ = 1.54184)
2Θ range for data collection/°	8.714 to 141.928
Index ranges	-25 ≤ h ≤ 25, -13 ≤ k ≤ 13, -21 ≤ l ≤ 15
Reflections collected	28096
Independent reflections	7529 [Rint = 0.0345, Rsigma = 0.0264]
Data/restraints/parameters	7529/0/527
Goodness-of-fit on F2	1.017
Final R indexes [I>=2σ (I)]	R1 = 0.0470, wR2 = 0.1270
Final R indexes [all data]	R1 = 0.0519, wR2 = 0.1332
Largest diff. peak/hole / e Å-3	0.39/-0.40

- **Cu^{I}(1)(Cl)** (CCDC 1951500)

Single crystals of $C_{45}H_{42}ClCuN_4O_6$ (**Cu^{I}(1)(Cl)**) were crystallized by slow diffusion of Et_2O in a CH_2Cl_2 solution of the compound. A suitable crystal was selected and mounted on a SuperNova, Dual, Cu at home/near, AtlasS2 diffractometer. The crystal was kept at 293 K during data collection. Using Olex2, [SX3] the structure was solved with the ShelXT, [SX4] structure solution program using Intrinsic Phasing and refined with the ShelXL, [SX5] refinement package using Least Squares minimisation.

Empirical formula	$C_{45}H_{42}ClCuN_4O_6$
Formula weight	833.81
Temperature/K	293
Crystal system	orthorhombic
Space group	$P2_12_12_1$
a/Å	11.7718(7)
b/Å	15.1157(8)
c/Å	21.9868(14)
Volume/Å3	3912.3(4)
Z	4

ρcalcg/cm3	1.416
μ/mm-1	0.682
F(000)	1736.0
Crystal size/mm3	0.44 × 0.3 × 0.14
Radiation	MoKα (λ = 0.71073)
2Θ range for data collection/°	5.742 to 55.724
Index ranges	-15 ≤ h ≤ 9, -18 ≤ k ≤ 17, -28 ≤ l ≤ 18
Reflections collected	12359
Independent reflections	7513 [Rint = 0.0261, Rsigma = 0.0720]
Data/restraints/parameters	7513/0/518
Goodness-of-fit on F2	1.076
Final R indexes [I>=2σ (I)]	R1 = 0.0645, wR2 = 0.1423
Final R indexes [all data]	R1 = 0.1155, wR2 = 0.1658
Largest diff. peak/hole / e Å-3	0.93/-0.45
Flack parameter	0.48(3)

Chiral HPLC resolution of (±)-1

• The sample is dissolved in chloroform, injected on the chiral column, and detected with an UV detector at 254 nm and circular dichroism detector at 254 nm. The flow-rate is 1 mL/min.

Column	Mobile Phase	t1	k1	t2	k2	α	Rs
Chiralpak ID	Heptane / ethanol and triethylamine / dichloromethane (30/30/40)	5.36 (-)	0.82	6.76 (+)	1.29	1.58	4.40

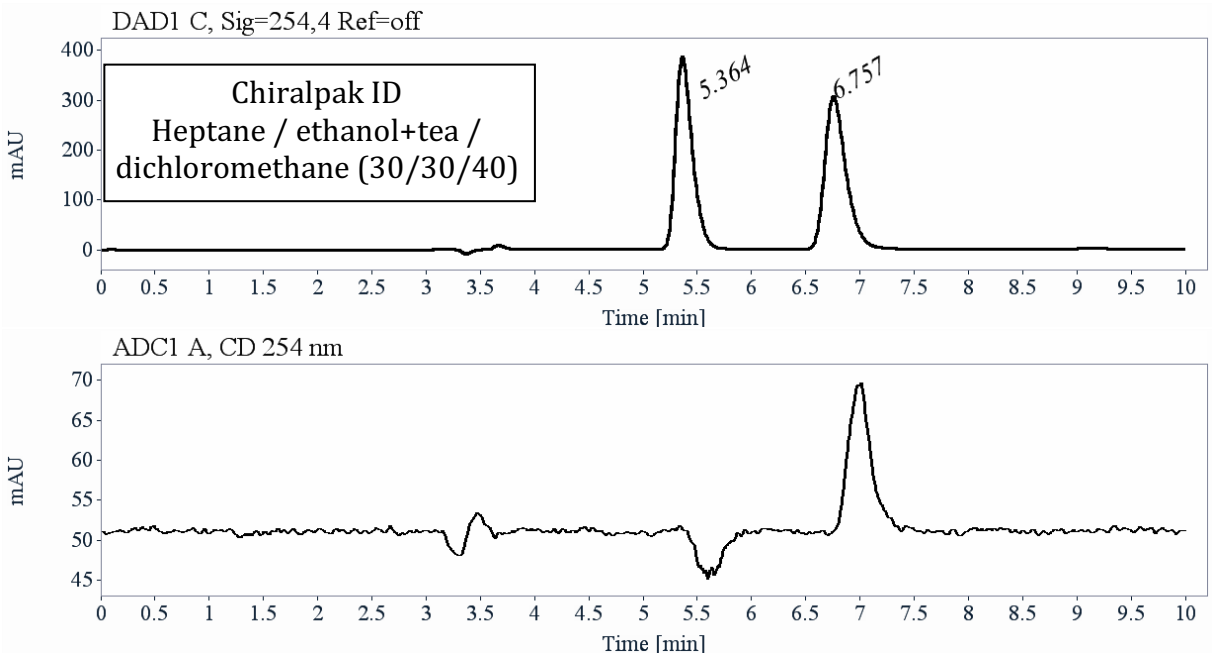

RT [min]	Area	Area%	Capacity Factor	Enantioselectivity	Resolution (USP)
5.36	4183	50.08	0.82		
6.76	4169	49.92	1.29	1.58	4.40
Sum	8352	100.00			

Preparative separation for **1** :

• Sample preparation: About 38 mg of **1** are dissolved in 2 mL of dichloromethane.

• Chromatographic conditions: Chiralpak ID (250 x 10 mm), hexane / ethanol and triethylamine / dichloromethane (30/30/40) as mobile phase, flow-rate = 5 mL/min, UV detection at 254 nm.

• Injections (stacked): 4 times 500 µL, every 7.2 minutes.

• First fraction: 13 mg of the first eluted with ee > 99.5 %

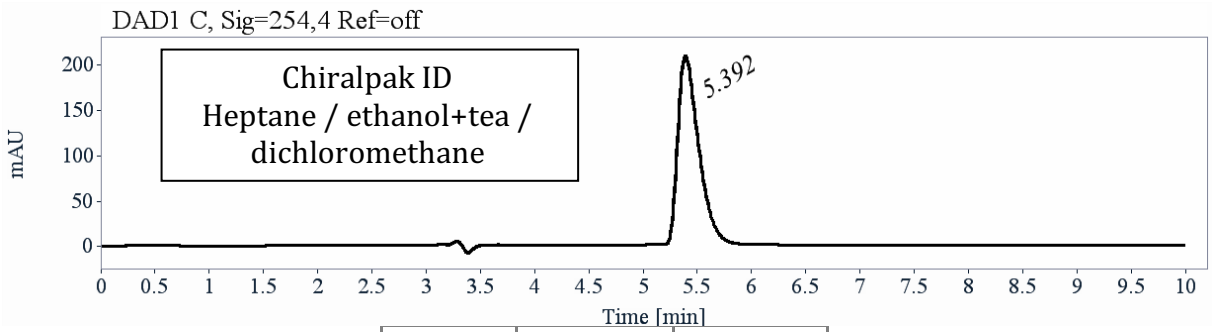

RT [min]	Area	Area%
5.39	2785	100.00
Sum	2785	100.00

• Second fraction: 13 mg of the second eluted with ee > 99.5%

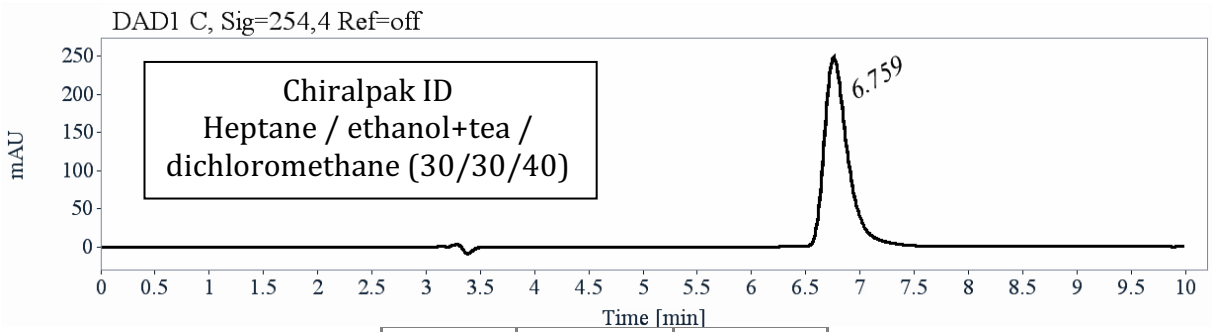

RT [min]	Area	Area%
6.76	3605	100.00
Sum	3605	100.00

Optical rotations

Optical rotations were measured on a Jasco P-2000 polarimeter with a halogen lamp (589, 578, 546, 436, 405 and 365 nm), in a 10 cm cell, thermostated at 25°C with a Peltier controlled cell holder.

λ (nm)	**1** first eluted on Chiralpak ID $[\alpha]_\lambda^{25}$ (CH_2Cl_2, c = 0.170)	**1** second eluted on Chiralpak ID $[\alpha]_\lambda^{25}$ (CH_2Cl_2, c = 0.171)
589	- 168	+ 168
578	-176	+ 176
546	- 205	+ 205
436	- 364	+ 363
405	- 455	+ 456
365	- 657	+ 656

Supplementary figures

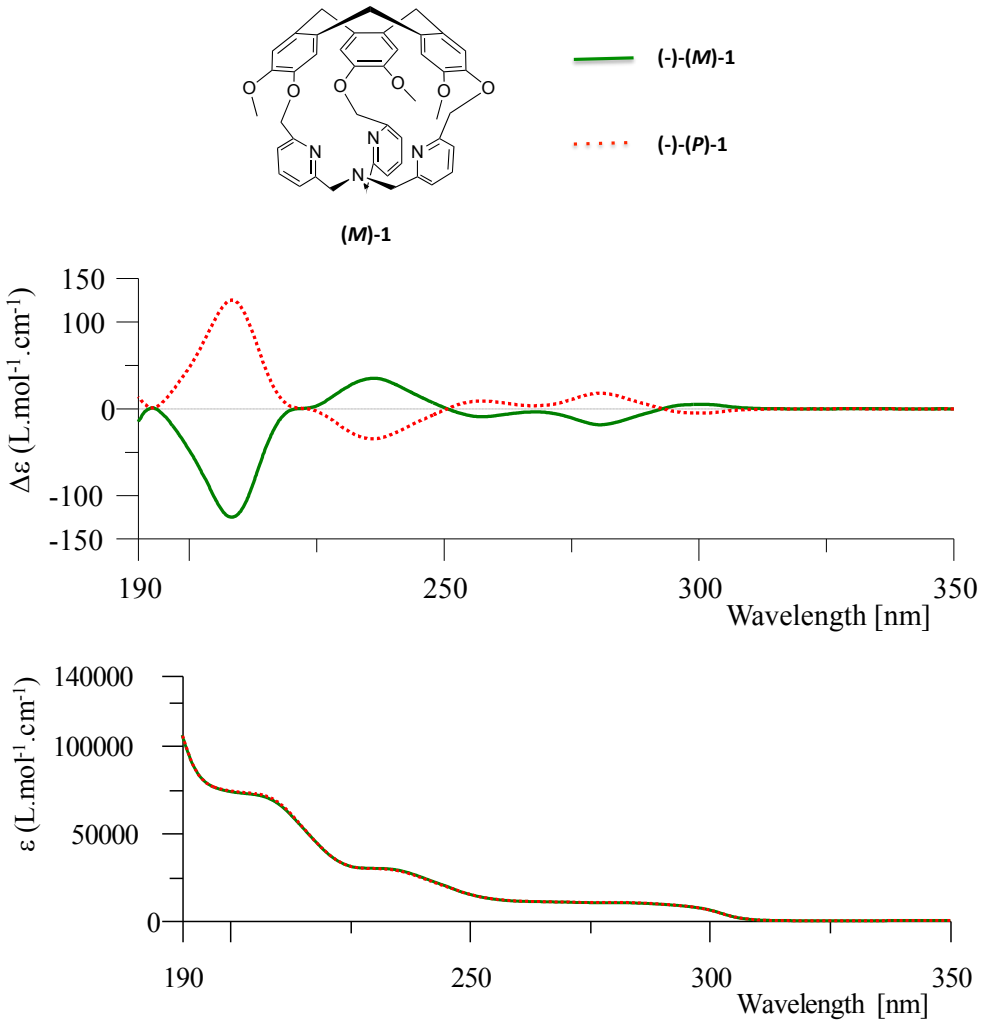

Figure S1. ECD (top) and UV (bottom) spectra of **(-)-1** and **(+)-1**. First eluted enantiomer **(-)-1** : green solid line (0.132 mM in CH_3CN). Second eluted enantiomer **(+)-1** : red dotted line, (0.148 mM in CH_3CN). Acquisition parameters: 0.1 nm as intervals, scanning speed 50 nm/min, band width 2 nm, and 3 accumulations per sample.

Absolute configuration assignement:

The spectra of the first eluted enantiomer exhibit a characteristic positive-negative bisignate curve from 230 to 250 nm corresponding to the *M*-configuration.[S6] A mirrored ECD signal is observed for the second eluted enantiomer attesting for its P-configuration. Indeed, according to Collet et al. the sign of the ^1L_a bands around 240nm can be used to assign the absolute configuration of the CTV unit because of its low sensitivity to the nature of substituents linked to the CTV part.[S6] The universal character of this assignment was confirmed by comparison with previsously reported *M* or *P* stereodescriptor of hemicryptophane analogues.[S7] Finally, the comparison between experimental and simulated ECD spectra of **(*M*)-1** (Figure S14 and S15) confirm this assignement. Therefore, according to both literature and ECD spectra calculations, the first eluted enantiomer on Chiralpak ID with $[\alpha]_D^{25}$ (CH_2Cl_2, c = 0.17) = -168, is the (*M*)-enantiomer.

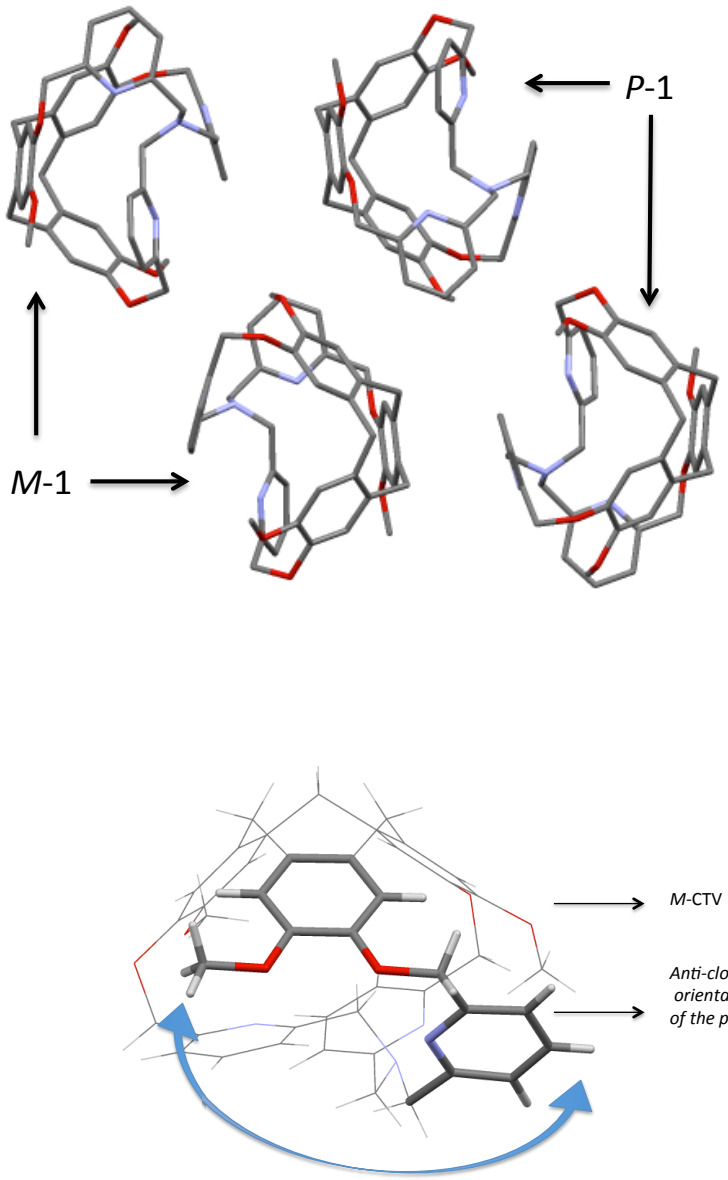

Figure S2. (Top) Crystal packing of **1** showing the presence of the two enantiomers **(*M*)-1** and **(*P*)-1**.
(Bottom) Diagram of the XRD structure of **(*M*)-1**, highlighting the rotation of the pyridines away from the closest CTV's -OMe group; resulting in they anti-clockwise orientation. The putative structure in which a clockwise arrangement of the pyridines is placed in the *M*-CTV environment (rotation of the pyridine toward -OMe group) can not be observed, probably because it will cause additional strain.

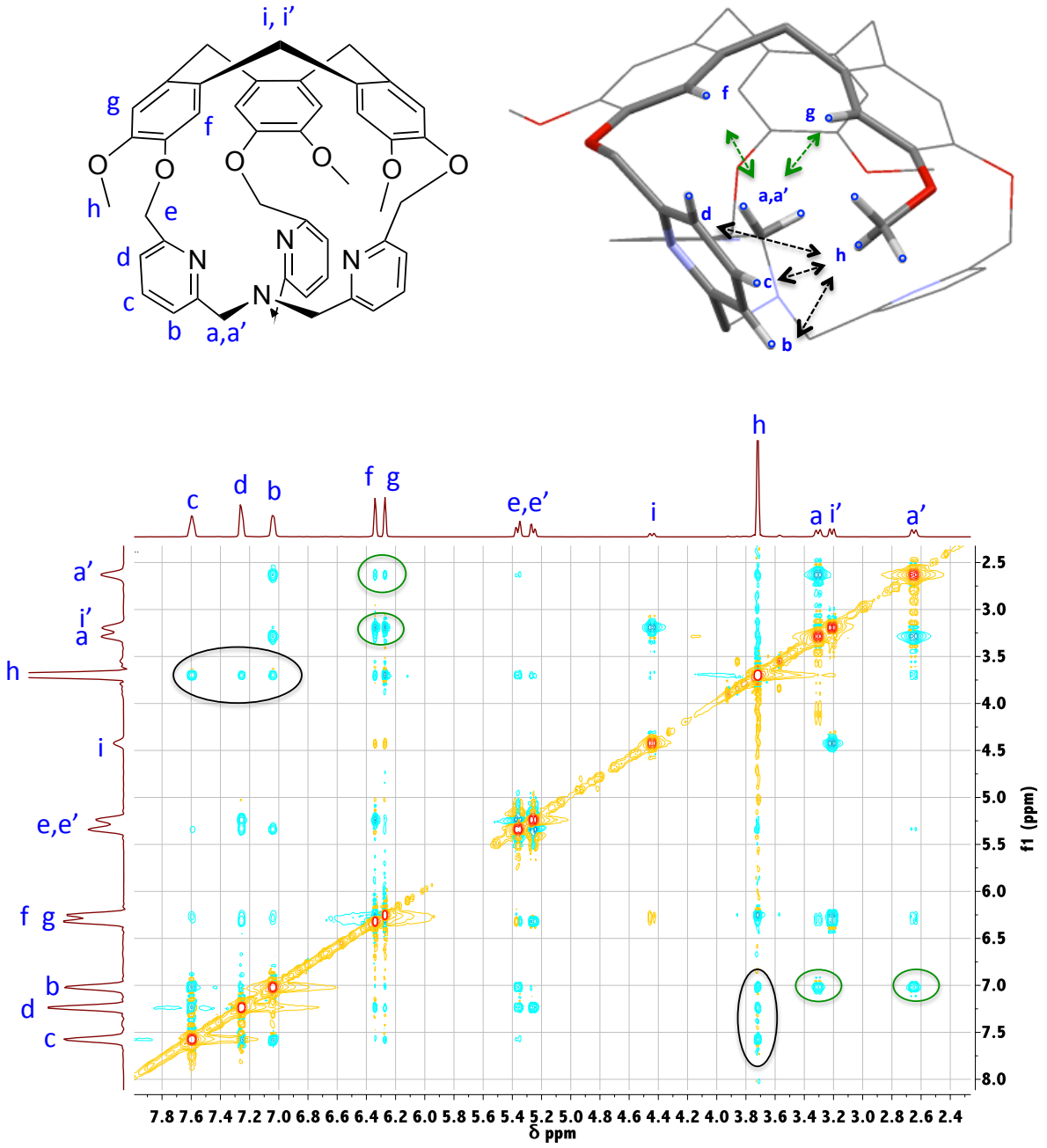

Figure S3. 2D NOESY spectrum (500MHz; mixing time of 500ms) of **1** in $CDCl_3$, at 298K. In the *C_1* symetrical conformation of **1** observed in solid state (top right), the imposed torsion and orientation of all pyridines give distances H_c(pyridine)…H_h(OMe) of 2.40 Å, 2.56 Å and 3.21 Å for the three pyridines (Fig. S4), which are consistent with the experimentally observed NOE (Same for H_a...H_f and $H_{a'}$..H_g which respectively display distances of 3.12 Å and 3.68 Å).
On the contrary, in the putative *C_3* symetrical conformation of **1** (top left), the methylene protons –**CH_2**-N ($H_{a,a'}$) are pointing outward (away from the CTV unit), excluding any through-space correlation with H_f and H_g protons.

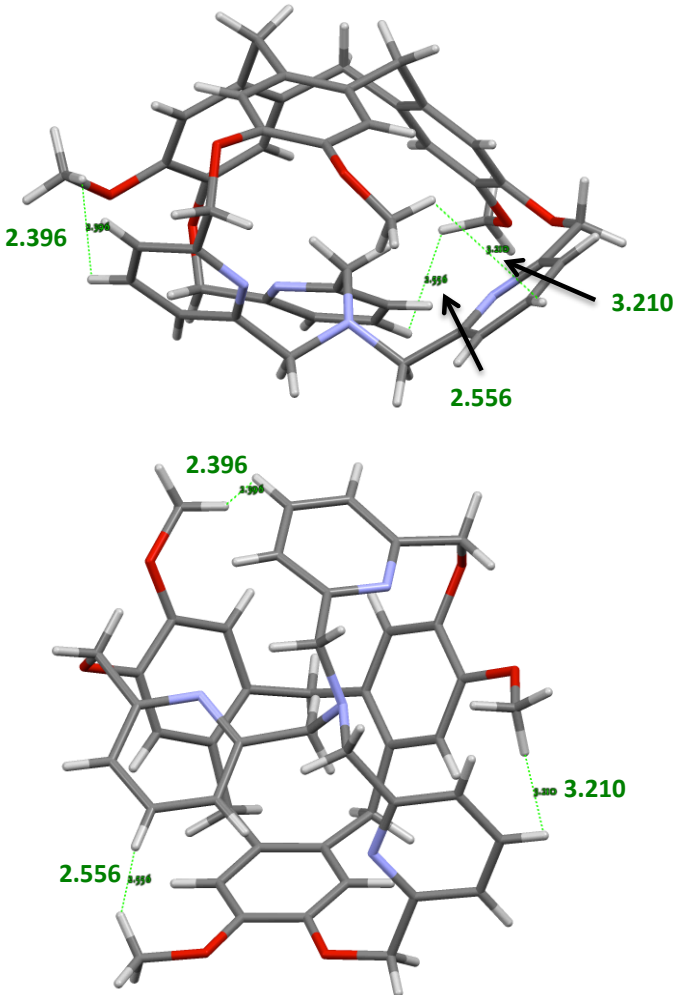

Figure S4. Side (top) and south views (bottom) of the XRD structure of ***P*-1**. Distances between H_c proton (Å) of the pyridines and the closest $-OCH_3$ proton of CTV unit are depicted in green.

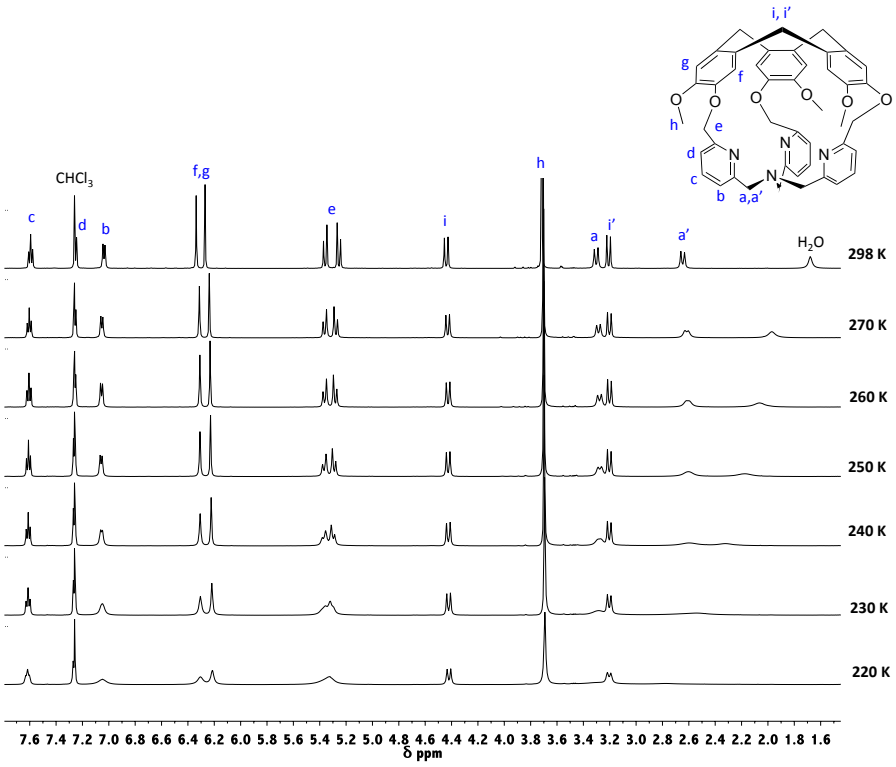

Figure S5. Temperature dependence of the ^{1}H-NMR spectra (500 MHz, $CDCl_3$) of **1** from 298 to 220K.

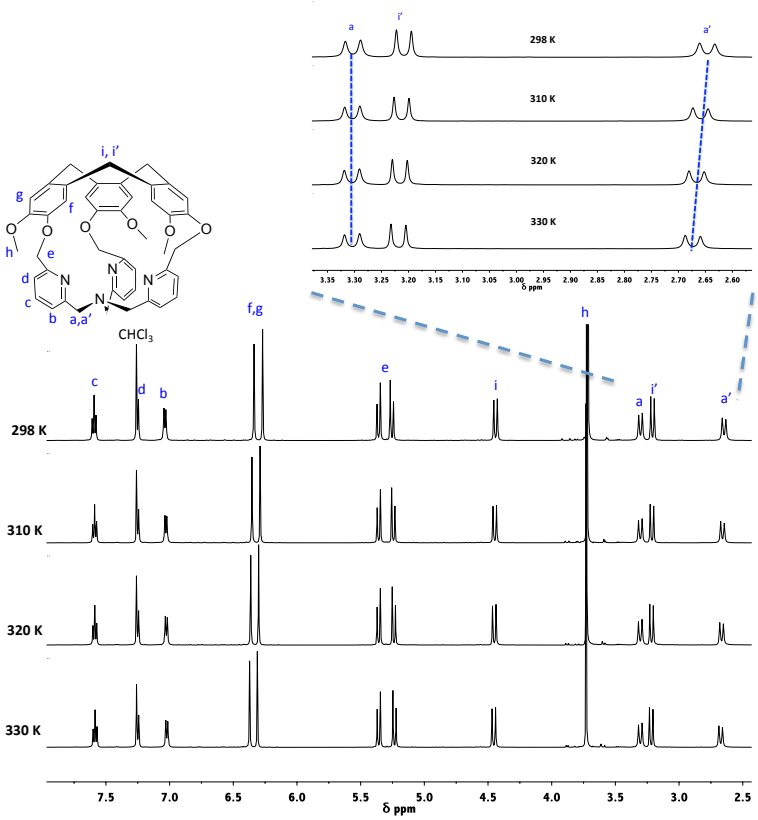

Figure S6. Temperature dependence of the ^{1}H-NMR spectra (500 MHz, $CDCl_3$) of **1** from 298 to 330K.

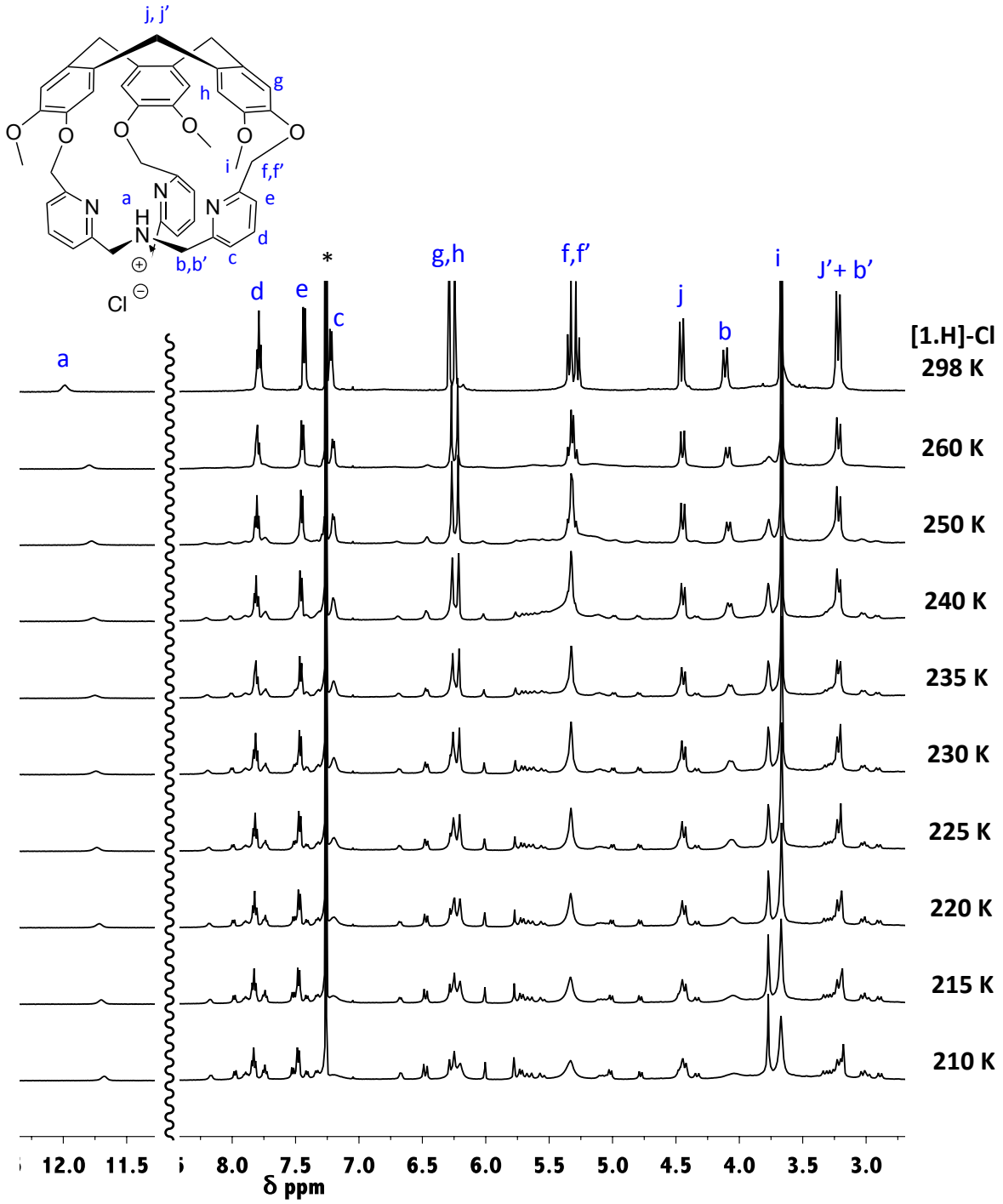

Figure S7. Temperature dependence of the ^{1}H-NMR spectra (500 MHz, $CDCl_3$) of **[1.H]-Cl** from 210 to 298K.

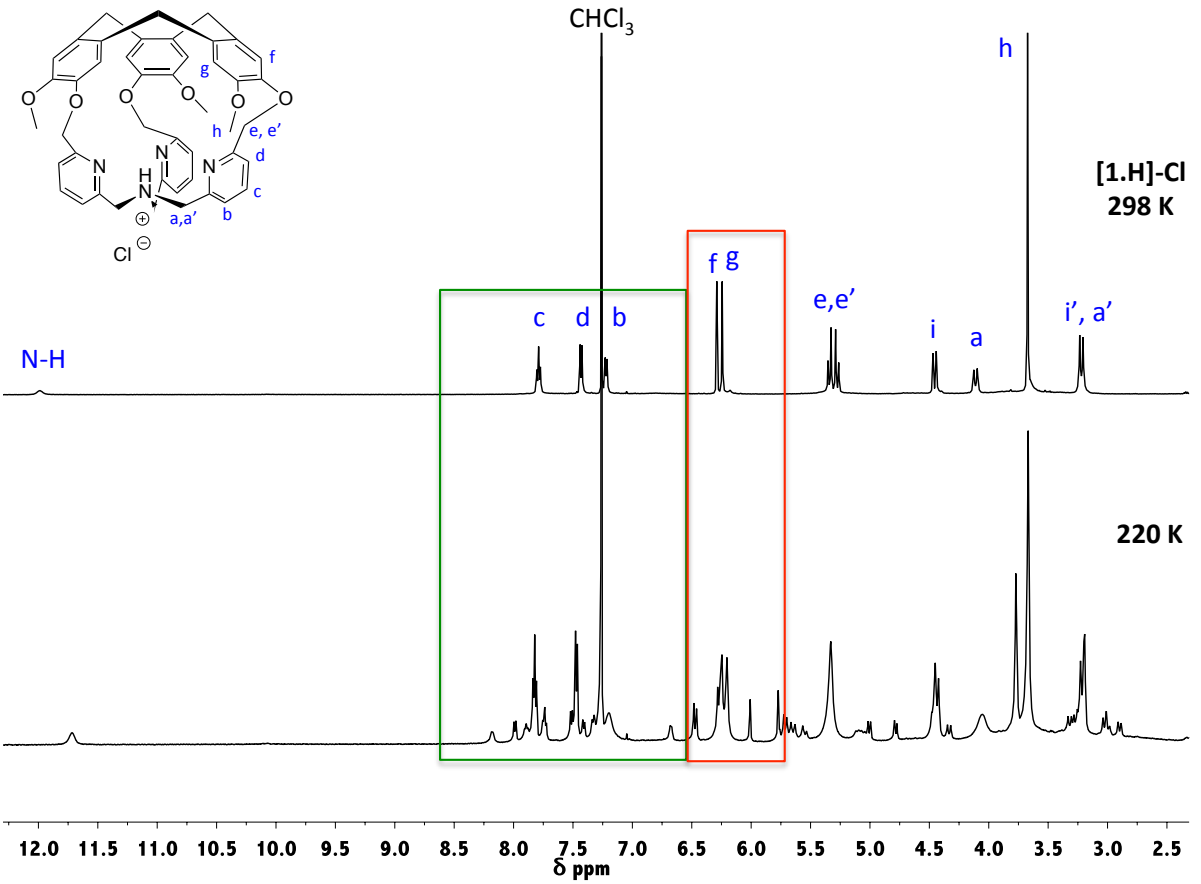

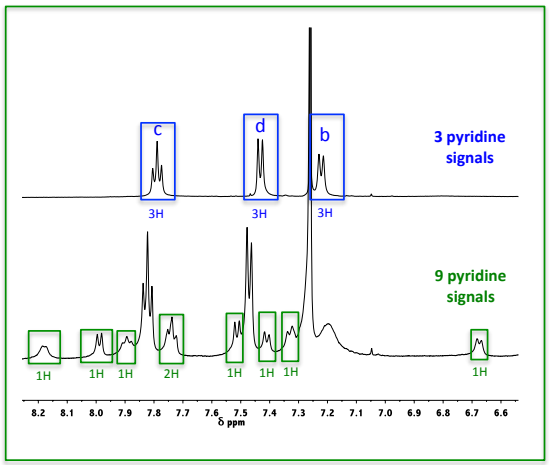

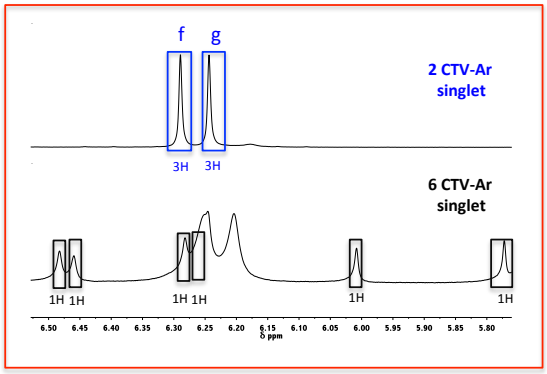

Figure S8. Comparison of the ^{1}H-NMR spectra ($CDCl_3$, 500 MHz) of **[1.H]-Cl** at 298K and 220K (top). Zoom on the region 6.6-8.2 ppm and 5.80-6.5 ppm showing the appearance of signal corresponding to the C_1 symmetrical form of **1** at lower temperature.

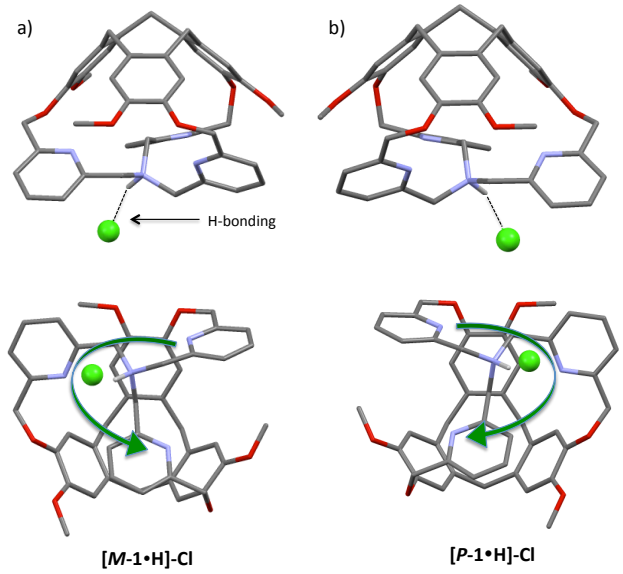

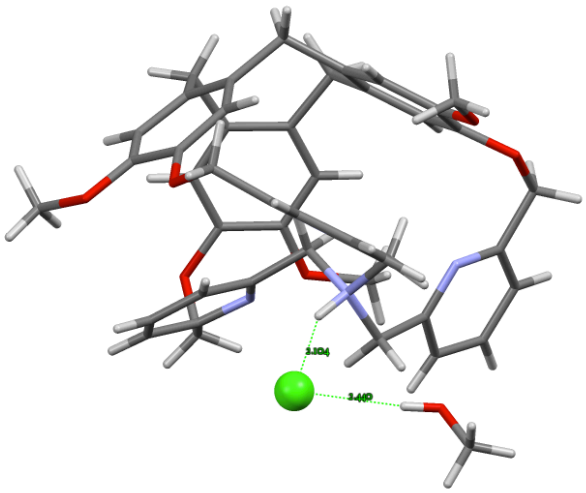

[*M*-1•H]-Cl

Figure S9. Top : Side and south views of the X-ray crystal structure of the protonated capsule **[1.H]-Cl** displaying **[*M*-1.H]-Cl** (a) and **[*P*-1.H]-Cl** (b) enantiomers. Only hydrogen atom belonging to the protonated tertiary amine has been included for clarity.

Bottom: Diagram of the X-ray crystal structure of **[1.H]-Cl**, only the *M* enantiomer is represented. The chlorine anion appear in close contact with both the protonated tertiary amine of **1** ($D_{N\text{-}H\text{--}Cl}$= 2.104 Å, $\Theta_{N\text{-}H\text{—}Cl}$ = 153.29°) and an exogeneous molecule of MeOH ($D_{O\text{-}H\text{--}Cl}$ = 2.440 Å, $\Theta_{O\text{-}H\text{—}Cl}$ = 159.47°).

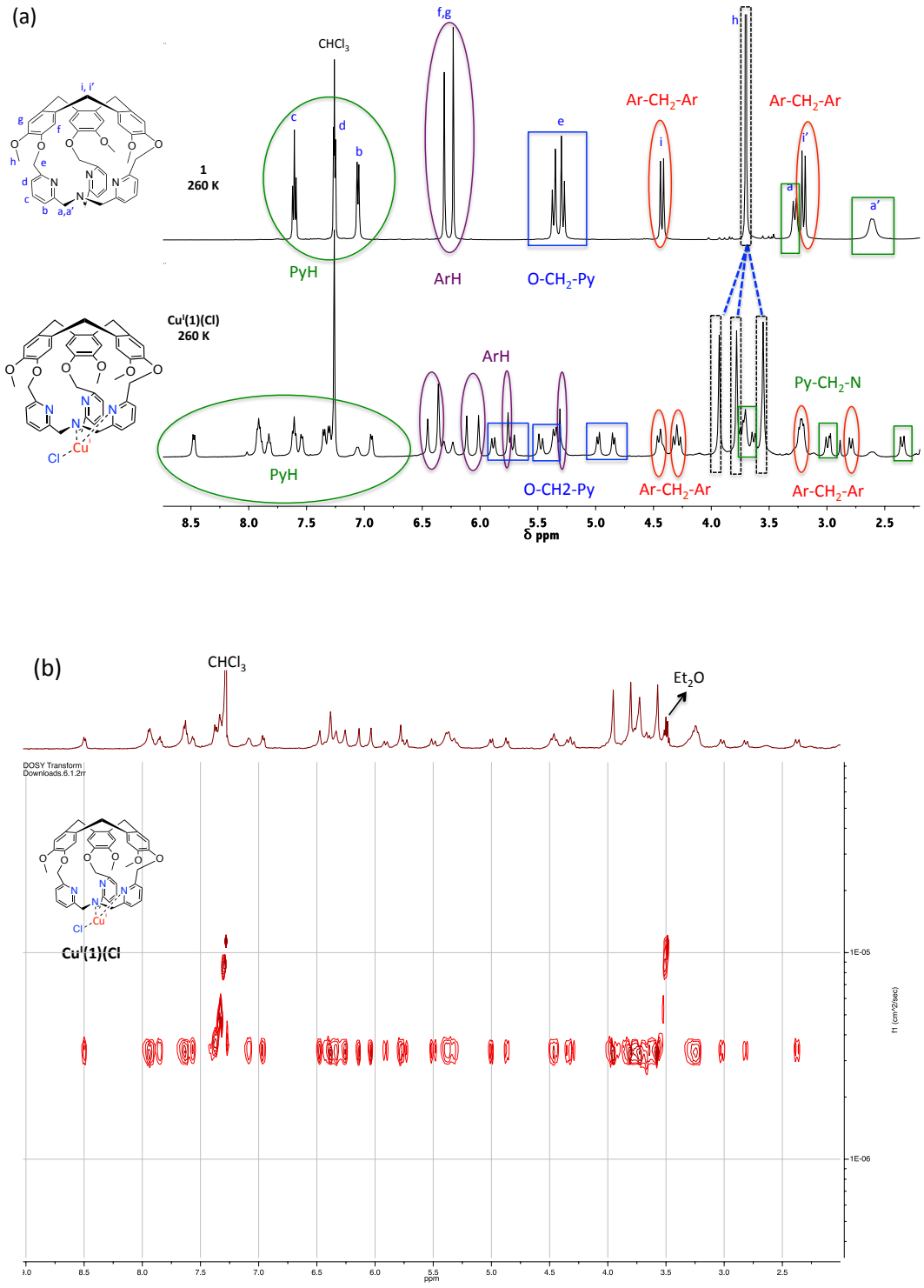

Figure S10. (a) Comparison of the ^{1}H NMR spectra (260K, $CDCl_3$, 500 MHz) of **1** (top) and **Cu^{I}(1)(Cl)** (bottom). Compared to **1** all proton signals belonging to **Cu^{I}(1)(Cl)** appear tripled attesting for the retention of the C_1 symmetrical structure observed in the DRX structure (see figure 7 main text). (b) 2D-DOSY NMR spectrum (500 MHz) of **Cu^{I}(1)(Cl** in $CDCl_3$ at 260K, all signals assigned to **Cu^{I}(1)(Cl** in the range 8.5-2.0 ppm have identical diffusion coefficient. The DOSY spectra of **Cu^{I}(1)(Cl** afford a diffusion coefficient of D= $3.74.10^{-10}$ m^2s^{-1} (fitted function f (x) = Io * exp (-D * x^2 * gamma^2 * littleDelta^2 (bigDelta-littleDelta/3)* 10^4 ; little delta= 0.003 s, big delta= 0.0754 s.

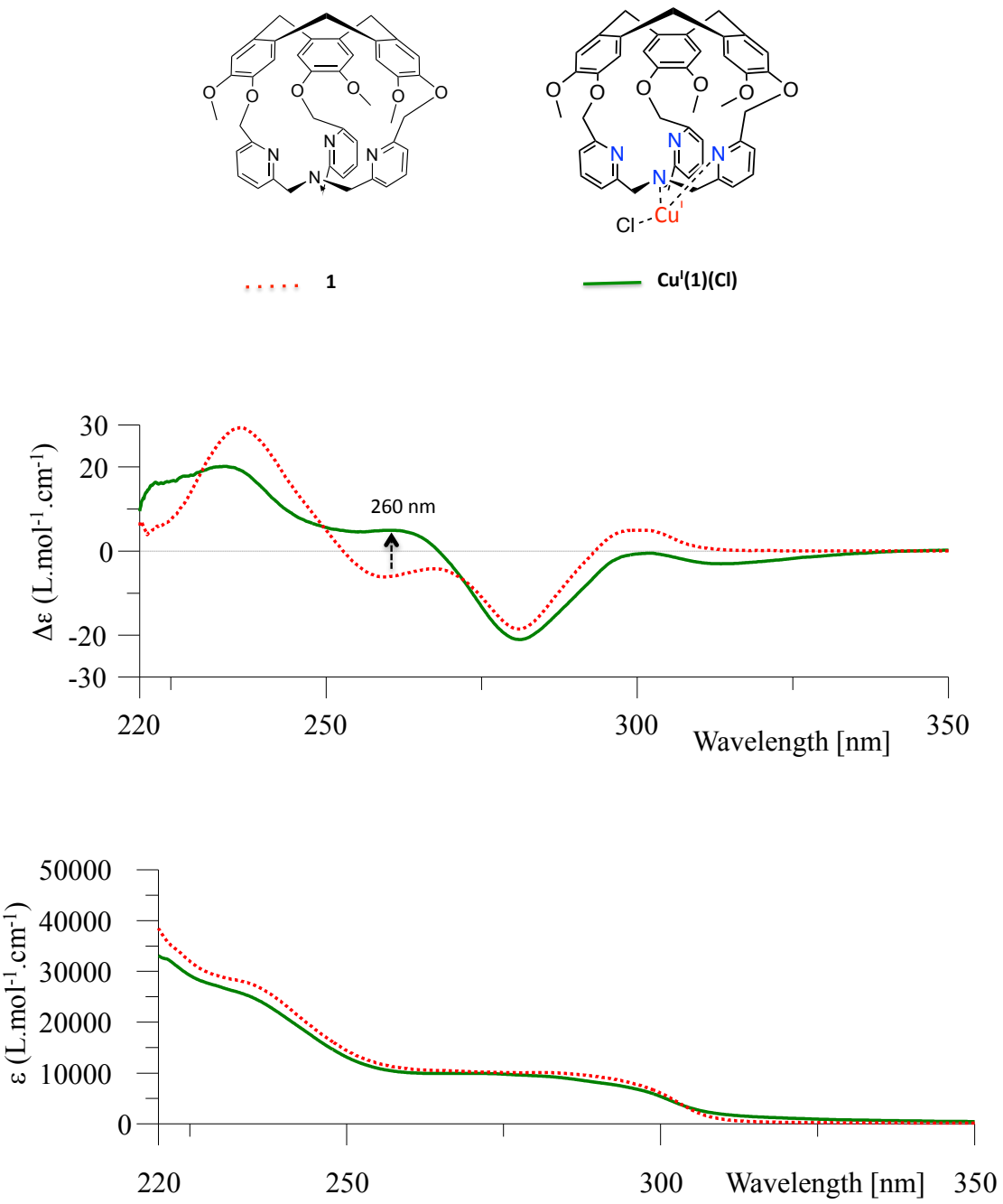

Figure S11. ECD (top) and UV (bottom) spectra of **(*M*)-Cu(1)Cl** (green solid line, 0,512mM in CH_2Cl_2), and **(*M*)-1** (red dotted line, 0,569mM in CH_2Cl_2).

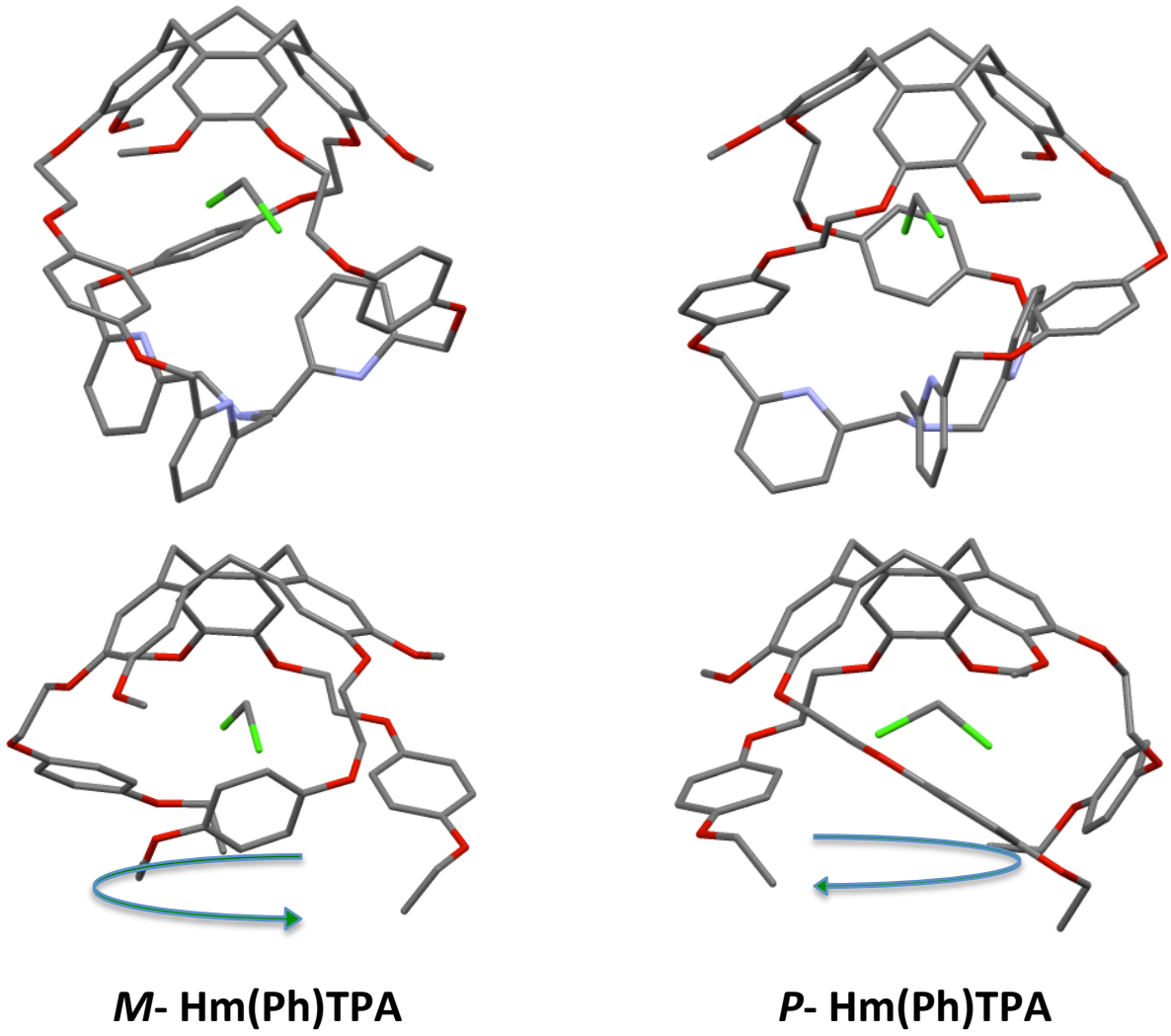

Figure S12. Representation of the XRD structure of **Hm(Ph)TPA** (top),[S8] same structure with omitted southern TPA unit for clarity (bottom). Structures of the (*M*-) and (*P*-) enantiomers of **Hm(Ph)TPA** are represented. A triple-stranded helical arrangement of the phenyl linkers is observed. No propeller orientation of the TPA moiety could be observed

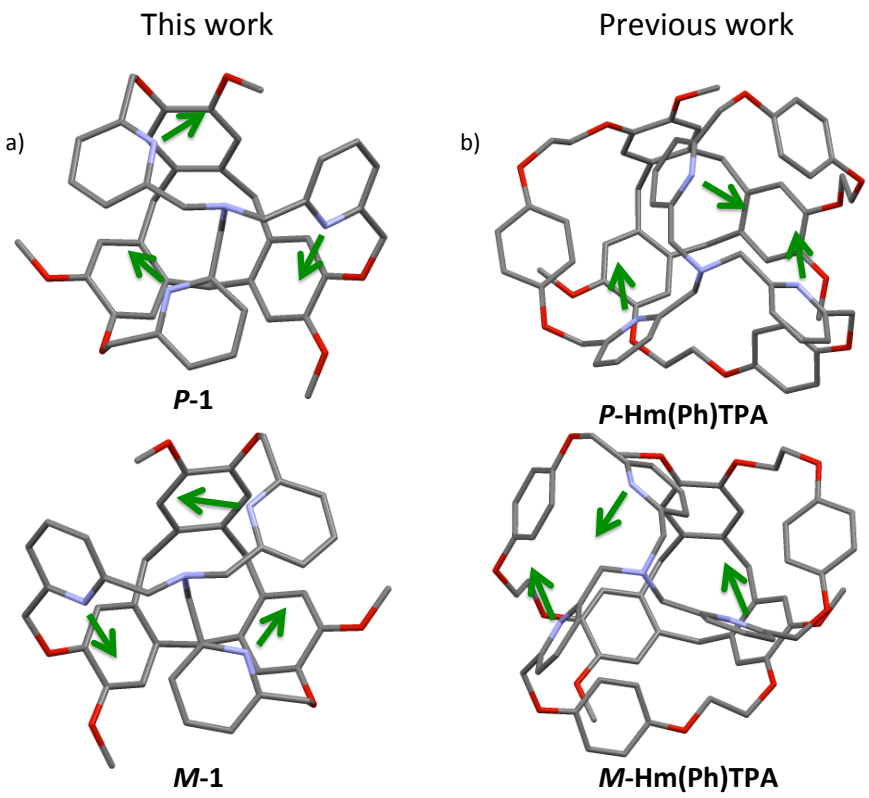

Figure S13. View from the south-north axis of the XRD structure of **1** (a) and **Hm-Ph-TPA,**[S8] (b). Both *P*- (top) and *M*- (bottom) enantiomers are depicted. Green arrows represent the orientation of the pyridine units. Unlike **1**, no propeller-like orientation of the pyridines could be observed in the case of **Hm-Ph-TPA**. Entrapped CH_2Cl_2 solvent molecule is omitted in the case of **Hm-Ph-TPA** for clarity.

4. Calculations

DFT and TD-DFT calculations were performed using Gaussian 16 package,[S9] with the default parameters for solvent used in SMD. Spectra were plotted with Specdis v. 1.71[S9] as sum of Gaussians with σ as half the bandwidth at $1/e$ peak height.
Calculations were done on the geometry obtained by X-ray analysis. The (*M*)-enantiomer was calculated.

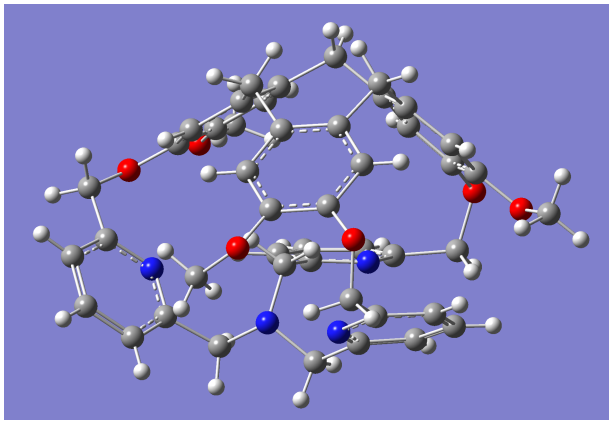

1) TD-DFT calculations at SMD(CH_3CN)/LC-ωhPBE/Def2SVPP level : 120 excited stated were computed.

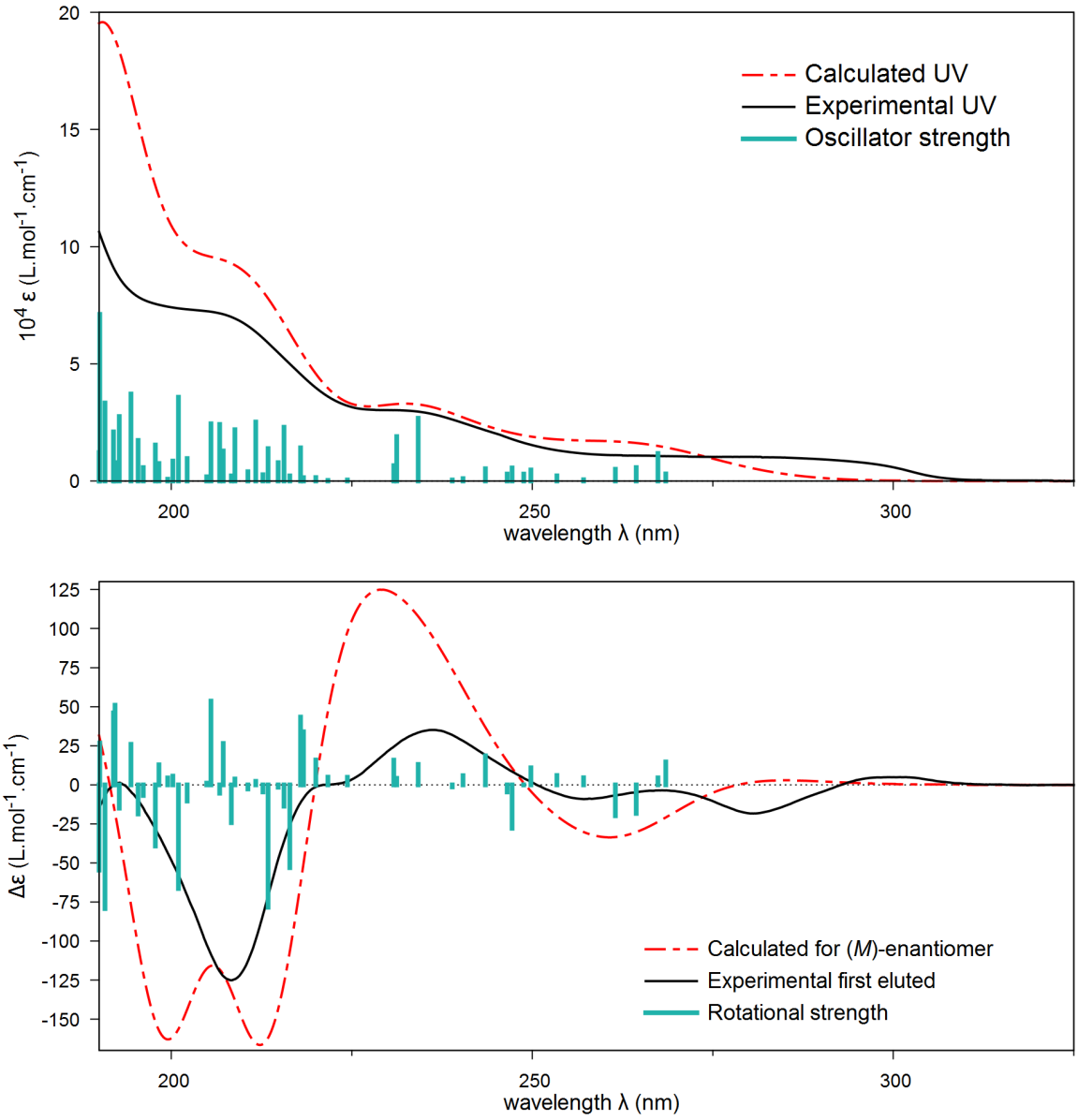

Figure S14. Comparison of UV (top) and ECD (bottom) experimental spectra in acetonitrile for the first eluted enantiomer on Chiralpak ID and TD-DFT calculated spectra (σ = 0.30 eV, shifted by 24 nm). Vertical bars are oscillator and rotational strengths calculated for the two conformers with arbitrary unit.

2) TD-DFT calculations at SMD(CH_3CN)/CAM-B3LYP/6-31++g(d, p) level : 180 excited stated were computed.

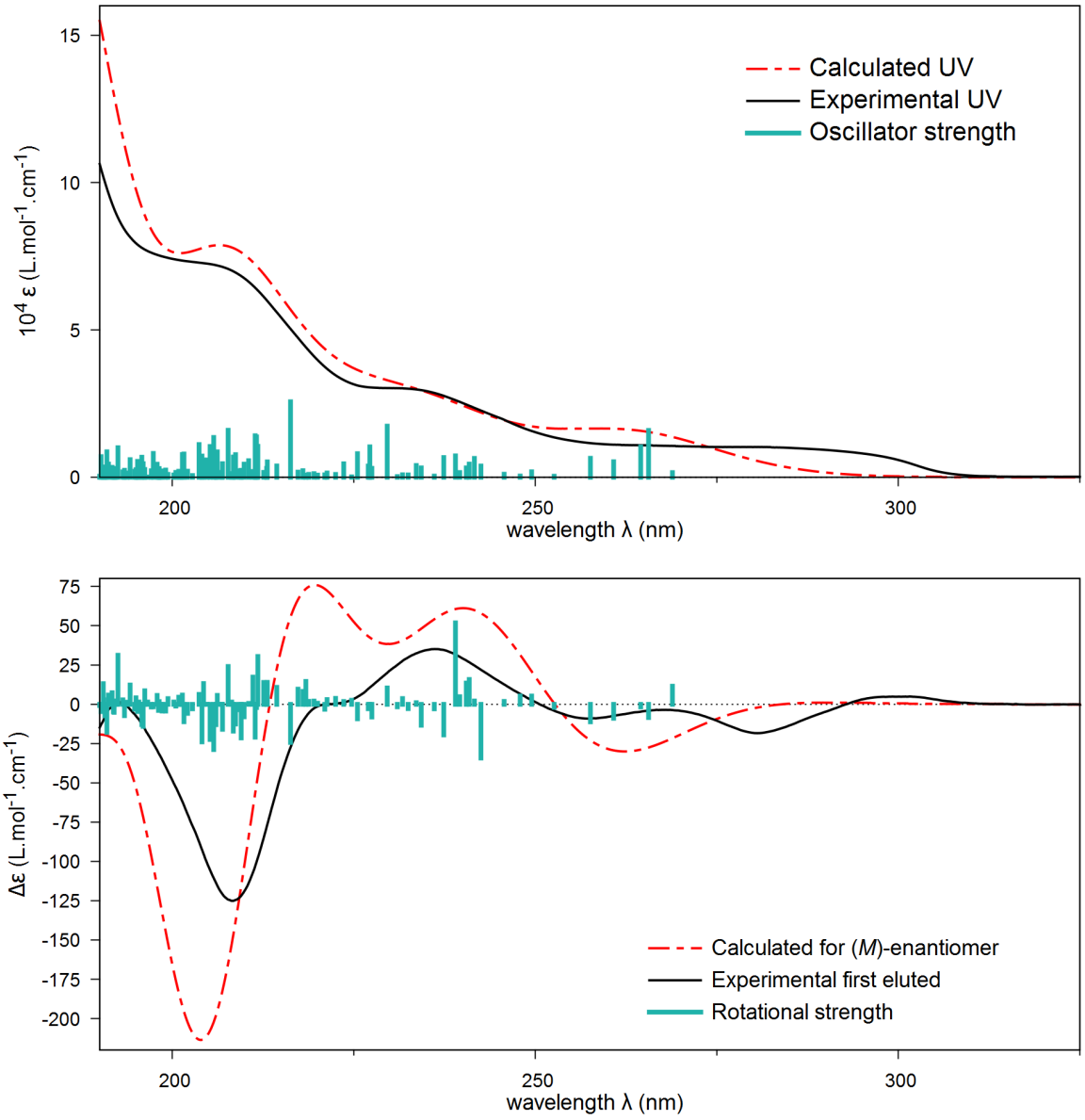

Figure S15. Comparison of UV (top) and ECD (bottom) experimental spectra in acetonitrile for the first eluted enantiomer on Chiralpak ID and TD-DFT calculated spectra (σ = 0.30 eV, shifted by 10 nm). Vertical bars are oscillator and rotational strengths calculated for the two conformers with arbitrary unit.

According to both above ECD spectra calculations, the first eluted enantiomer on Chiralpak ID with $[\alpha]_D^{25}$ (CH_2Cl_2, c = 0.17) = - 168, is the (*M*)-enantiomer.

5. Acknowledgements:

Calculations were supported by the computing facilities of the CRCMM, '*Centre Régional de Compétences en Modélisation Moléculaire de Marseille'*. We thank spectropole and Mme R. Rosas for NMR assistance.

6. Supplementary references.

[S1] D. Zhang, B. Bousquet, J. C. Mulatier, D. Pitrat, M. Jean, N. Vanthuyne, L. Guy, J. P. Dutasta and A. Martinez, *J. Org. Chem.*, 2017, 82, 6082- 6088

[S2] T.Brotin, V. Roy and J. P. Dutasta, *J. Org. Chem.*, 2005, **70**, 6187-6195

[S3] O. V. Dolomanov, L. J. Bourhis, R. J. Gildea, J. A. K. Howard, H. J. Puschmann, *Appl. Cryst.,* 2009, **42**, 339-341.

[S4] G. M. Sheldrick, *ActaCryst.*, 2015, **A71**, 3-8.

[S5] G. M. Sheldrick, *ActaCryst.* 2015, **C71**, 3-8.

[S6](a) A. Schmitt, O. Perraud, E. Payet, B. Chatelet, B. Bousquet, M. Valls, D. Padula, L. Di Bari, J. P. Dutasta, A. Martinez, *Org. Biomol. Chem.*, 2014, **12**, 4211. (b) O. Perraud, P. Dimitrov-Raytchev, A. Martinez, J. P. Dutasta, *Chirality*, 2010, **22,** 88. (c) J. R. Cochrane, A. Schmitt, U. Wille, C. A. Hutton, *Chem. Commun.*, 2013, **49**, 8504. (d) J. Canceill, A. Collet, J. Gabard, G. Gottarelli, G. P. Spada, *J. Am. Chem. Soc.*, 1985, **107**, 1299. (e) J. Canceill, A. Collet, G. Gottarelli, P. Palmieri, *J. Am. Chem. Soc.*, 1987, **109**, 6454.)

[S7] Ł. Szyszka, P. Cmoch, A. Butkiewicz, M. A. Potopnyk, S. Jarosz, *Org. Lett.* 2019, **21**, 6523−6528

[S8] S. A. Ikbal, C. Colomban, D. Zhang, M. Delecluse, T. Brotin, V. Dufaud, J. P. Dutasta, A. B. Sorokin and A. Martinez, *Inorg. Chem.*, 2019, **58**, 7220-7228

[S9] (a) Gaussian 16, Revision A.03, M. J. Frisch, G. W. Trucks, H. B. Schlegel, G. E. Scuseria, M. A. Robb, J. R. Cheeseman, G. Scalmani, V. Barone, G. A. Petersson, H. Nakatsuji, X. Li, M. Caricato, A. V. Marenich, J. Bloino, B. G. Janesko, R. Gomperts, B. Mennucci, H. P. Hratchian, J. V. Ortiz, A. F. Izmaylov, J. L. Sonnenberg, D. Williams-Young, F. Ding, F. Lipparini, F. Egidi, J. Goings, B. Peng, A. Petrone, T. Henderson, D. Ranasinghe, V. G. Zakrzewski, J. Gao, N. Rega, G. Zheng, W. Liang, M. Hada, M. Ehara, K. Toyota, R. Fukuda, J. Hasegawa, M. Ishida, T. Nakajima, Y. Honda, O. Kitao, H. Nakai, T. Vreven, K. Throssell, J. A. Montgomery, Jr., J. E. Peralta, F. Ogliaro, M. J. Bearpark, J. J. Heyd, E. N. Brothers, K. N. Kudin, V. N. Staroverov, T. A. Keith, R. Kobayashi, J. Normand, K. Raghavachari, A. P. Rendell, J. C. Burant, S. S. Iyengar, J. Tomasi, M. Cossi, J. M. Millam, M. Klene, C. Adamo, R. Cammi, J. W. Ochterski, R. L. Martin, K. Morokuma, O. Farkas, J. B. Foresman, and D. J. Fox, Gaussian, Inc., Wallingford CT, **2016**.
(b) Specdis version 1.71. T. Bruhn, A. Schaumlöffel, Y. Hemberger, G. Pescitelli. Berlin, Germany, **2017**, https://specdis-software.jimdo.com/.